*Desalination and Water Treatment*
www.deswater.com

doi: 10.1080/19443994.2013.768376

51 (2013) 5097–5106
July

Taylor & Francis
Taylor & Francis Group

# Studies of supported phospholipid bilayers formed on nanofiltration membranes surface

Zhining Wang*, Zhilei Zhang, Xida Wang, Li Wang, Miaoqi Wang, Shuzheng Wang, Jinyu Sheng, Tao Wang, Xingchen Liu, Congjie Gao

*Key Laboratory of Marine Chemistry Theory and Technology of Ministry of Education, College of Chemistry and Chemical Engineering, Ocean University of China, Qingdao 266100, China*
*Tel. +86 532 66782017; Fax: +86 532 66782301; email: wangzhn@ouc.edu.cn*

Received 2 June 2012; Accepted 28 September 2012

ABSTRACT

Reverse osmosis (RO) is currently the most important desalination technology and it is experiencing significant growth. However, the developments of membrane permselectivity in the past decade have been relatively slow, and membrane fouling remains a severe problem. The excellent water transport properties of biological membranes with specialized transmembrane proteins aquaporins as water-selective channels exceed those commercial membranes for water desalination. Supported phospholipid bilayers (SPBs) can maintain the biological activity of molecules and inhibit other non-specific adsorption of biological molecules. In this study, the main work is mostly focused on conditions ensuring most efficient coverage of the supporting nanofiltration (NF) membranes with phospholipid bilayers. Four different NF membranes as supports are explored to form phospholipid bilayers. The presence of SPBs on the four different NF membranes surface is verified and quantified by atomic force microscope (AFM), attenuated total reflection Fourier transform infrared (ATR-FTIR) and contact angle measurements techniques. The NTR-7450 surface is noticeably smoother, more homogeneous and hydrophobicity. Meanwhile, the top layer of NTR-7450 membrane surface is dense and virtually impermeable to lipids and proteins. Therefore, it is shown that a defect-free SPBs is successfully formed on a NTR-7450.

*Keywords:* Desalination technology; Reverse osmosis; Supported phospholipid bilayers; Biomimetic membrane; Nanofiltration membranes

## 1. Introduction

Many worldwide problems associated with the lack of clean, fresh water are well known. Water crisis is expected to grow worse in the coming decades, with water scarcity occurring globally, even in regions currently considered water rich. Efficient desalination of sea and brackish water is one of the paths to solve the shortage of water resources in the worldwide. Reverse osmosis (RO) is the leading desalination technology at present. It has overtaken conventional thermal technology such as multi-stage flash (MSF) [1]. In the past few decades, different membrane materials

*Corresponding author.

*7th Aseanian Membrane Society Conference (AMS7), 4–7 July 2012, Busan, Korea*

have got significant development. Developing novel composite membrane materials is the research focus and development trend with the aim of reducing the energy consumption and achieving high efficiency, portable water purification technology in the desalination processes [2]. In AIChE Annual Meeting, Norman N. Li pointed out that the future trend of RO membrane is to modify the current membrane materials and achieve high flux, especially to design and prepare a brand-new reverse osmosis membrane, or put forward a new concept of RO membranes [3].

The biomembrane is one of the most important constituents in living organisms. It controls the transfer of information and the transport of ions and molecules by enclosing cells and separating their inner compartments, thereby enabling cells to contain isolated environments. The interest in understanding the properties of the biomembrane has spurred intense research to build simplified yet representative experimental model systems [4,5] with the aim to promote both fundamental understanding of membrane-related processes and utilization of them in synthetic systems. Supported phospholipid bilayers (SPBs) are popular models of cell membranes [6] for studying basic membrane processes and possible biotechnological applications [7,8]. Planar lipid bilayers were first developed for the investigation of the electrical properties described by Mueller et al. in the 1960s [9,10] and have since then aroused increasing scientific and practical attentions. The phospholipids are arranged in a bilayer, with their polar, hydrophilic phosphate heads facing outwards, and their non-polar, hydrophobic fatty acid tails facing each other in the middle of the bilayer. This hydrophobic layer acts as a barrier to all molecules, effectively isolating the two sides of the membrane.

Recently, nanocomposite membranes have become a research focus in membrane separation field, because it can overcome the "trade-off" effect of the traditional polymer membrane duo to the introduction of inorganic component in the polymer matrix. Mauter and Elimelech have discussed the perspective of carbon nanotube membranes as high-flux filters [11]. Carbon nanotubes (CNTs) have caught the attention of many researchers, due to the similarity between their fluid transport properties and those of water transport channels in biological membranes [12]. The excellent water transport properties of biological membranes have led to the study of membrane incorporating aquaporins, which are proteins functioning as water-selective channels in biological cell membranes [13]. Membranes incorporating bacterial Aquaporin Z proteins have been reported to show superior water transport efficiency relative to conventional RO membranes [14]. The functional biological performance of aquaporins is to only allow the passage of water molecules. Aquaporin (AQP) represents an ideal opportunity for the production of ultrapure water [15,16]. To support an almost defect-free surface coverage of a fluid bilayers, the substrates surface should be hydrophilic, smooth, and clean, such as mica, silicon, silica, etc. [17–19]. However, their impermeability renders them unsuitable for the desalination purpose. Also, a serious scientific and technological challenge is produced. The greatest challenge of current study is to design and prepare an effective barrier membrane, which allows the embedding of biological channels (such as AQP and CNTs) and sustains the hydraulic water pressure gradients without losing their integrity and performance [20]. Selective permeability of a water channel is essential for controlling the biochemical activities of a cell. It is important to choose a mechanically robust water permeable substrate to support the phospholipid bilayers. Hence, identification of appropriate support materials must be carried out to develop biomimetic membrane for practical use.

A new approach introduced and explored here is to prepare NF membranes supported lipid bilayers. The conventional NF composite membranes are made of a porous water-permeable polymer. Their surface has relatively low roughness [21,22], which minimizes possible distortions of the lipid bilayers and also facilitates the characterization. Their water permeability is high and commensurable with biological membranes. Meanwhile, they totally retain proteins and phospholipids. This article describes a part of the ongoing effort by our group about selecting the supporting substrate. Four different NF membranes surface can be optimized to favor good and continuous coverage with lipids.

## 2. Experimental section

### 2.1. Materials

Lipids and chemical: 1,2-Dioleoyl-sn-glycero-3-phosphocholine (DOPC) is obtained from Sigma-Aldrich. The material is used as received without further purification. The chemical structure of the lipid is shown in Fig. 1. Other materials such as chloroform (99.8%), tris (hydroxymethyl)-aminomethane

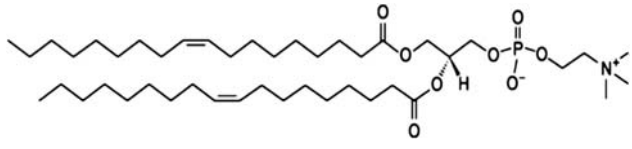

Fig. 1. Chemical structure of DOPC.

(Tris, 99.9%, Aldrich), sodium chloride (NaCl, 99.8%), and calcium chloride ($CaCl_2$) are of the highest purity available. Ultrapure water with a resistivity of 18.2 MΩ·cm is used.

Buffer solution: Milli-Q water (Barnstead, compact ultrapure water system) with a resistivity of 18.2 MΩ· cm is used for preparing Tris buffer containing 10 mM Tris, 150 mM NaCl, 10 mM $CaCl_2$, and the pH is adjusted to 8.0 with 1.0 M HCl solution.

NF membranes: NF270 and NF90 membranes are obtained from Dow-Filmtec; NTR7450 and NTR7250 membranes are kindly supplied from Hydranautics/ Nitto Denko. NF90 membrane and NF270 membrane are representative of the majority of commercial NF membranes. NF90 membrane is a metaphenylene diamine (MPD) product. NF270 membrane is a piperazine (PIP)-based NF membrane; its active layer is composed of cross-linked semi-aromatic polyamide also containing weakly acidic $COO^-$ groups and some amine groups [23,24]. NTR7250 membrane is a composite NF membrane that contains carbonyl and hydroxyl groups. NTR7450 membrane has an active layer made of sulfonated polyethersulfone that contains strongly acidic $SO_3^-$ group[25]. The membrane samples are immersed in sterile laboratory containers filled with 18.2 MΩ deionized water and stored at 4°C to minimize biological growth. Storage water is changed every week. Membrane samples are rinsed thoroughly with deionized water prior to use in experiments.

### 2.2. Methods

#### 2.2.1. Preparation of vesicles

A lipid film was prepared by evaporation of chloroform under a $N_2$ stream from a chloroform solution of DOPC. The lipid film was left standing overnight in a vacuum to remove the residual organic solvent and then resuspended in Tris buffer through vortexing, followed by five freeze-thaw cycles. Uniform small unilamellar vesicles (SUVs) were obtained by extrusion (11 times through 100 nm polycarbonate membranes) through an extruder system (Avanti Polar Lipids, Alabaster, AL).

#### 2.2.2. Substrate preparation

NF membranes are sonicated in ethanol/water (50/50 v/v) mixture solution for 10 min and then washed for 5 min in Milli-Q water. Deposition of a phospholipids bilayer is carried out by the method of vesicle fusion on the NF membrane.

#### 2.2.3. Atomic force microscopy (AFM)

AFM measurements are performed on a Multimode AFM with a Nanoscope V MultiMode controller (Veeco, USA) using manufacturer supplied software. Tapping mode measurements in liquid are performed using NP-S cantilevers (short lever, nominal spring constant 0.06 N/m). Roughness values (RMS) are obtained from topography scans using the instrument software.

#### 2.2.4. Attenuated total reflection Fourier transform infrared (ATR-FTIR)

FTIR spectra is recorded by the attenuated total refection (ATR) technique by using Bruker-Tensor 27 FTIR spectrometer (Bruker, Germany) to characterize the presence of functionalized groups in lipid (DOPC) structure and nanofiltration membranes. Each spectrum is recorded at a resolution of 4 $cm^{-1}$ in the range of 500–3,200 $cm^{-1}$ with 512 scans averaged for each spectrum.

#### 2.2.5. Contact angle measurements

The hydrophobicity/hydrophilicity of NF membranes and SPBs are characterized via static contact angle measurements, where the spreading of water droplets on the sample surface under ambient conditions is measured using the sessile drop technique [26,27]. A DSA 100 (Kruss, Germany) is used to perform the measurements. This device is equipped with a high-speed video camera to monitor the side images of the drop profile. Milli-Q water (3 μL) is injected onto a membrane surface using a microsyringe under ambient conditions. The contact angle is then measured after 10 s for the membranes and an average value is obtained by seven measurements for each membrane.

## 3. Results and discussion

### 3.1. Preparation of SPBs on mica

The ultimate purpose of our work is to demonstrate the formation of SPBs on permeable NF membranes surface, but the thickness of SPBs is only several nanometers. So it is essential to first explore its main conditions on mica as a benchmark substrate. AFM images of mica and SPBs on mica are listed in Fig. 2. Mica is widely used to characterize the formation of SPBs, as it is rigid, atomically smooth and non-fluorescent. Furthermore, mica as well as NF membranes exhibits significant negative surface charges [28].

Fig. 2(A) shows morphology of clean mica immersed in a buffer solution. The mica is fairly smooth and the roughness is 0.199 nm. The morphology of DOPC on mica is shown in Fig. 2(B). As observed from Fig. 2(B), the perfect SPBs have been formed on the surface of mica and the roughness of DOPC on mica is 0.287 nm. To certify the existence of SPBs on mica, the action force of AFM scanning is increased. It can be seen that the formed SPBs is damaged under high AFM scanning force, and the mica surface is exposed. The nick area of 1 μm × 1 μm is obtained (Fig. 2(C)). From the cross section image (Fig. 2(D)), it can be observed that the height of the DOPC bilayer is 4.323 nm. It is in good agreement

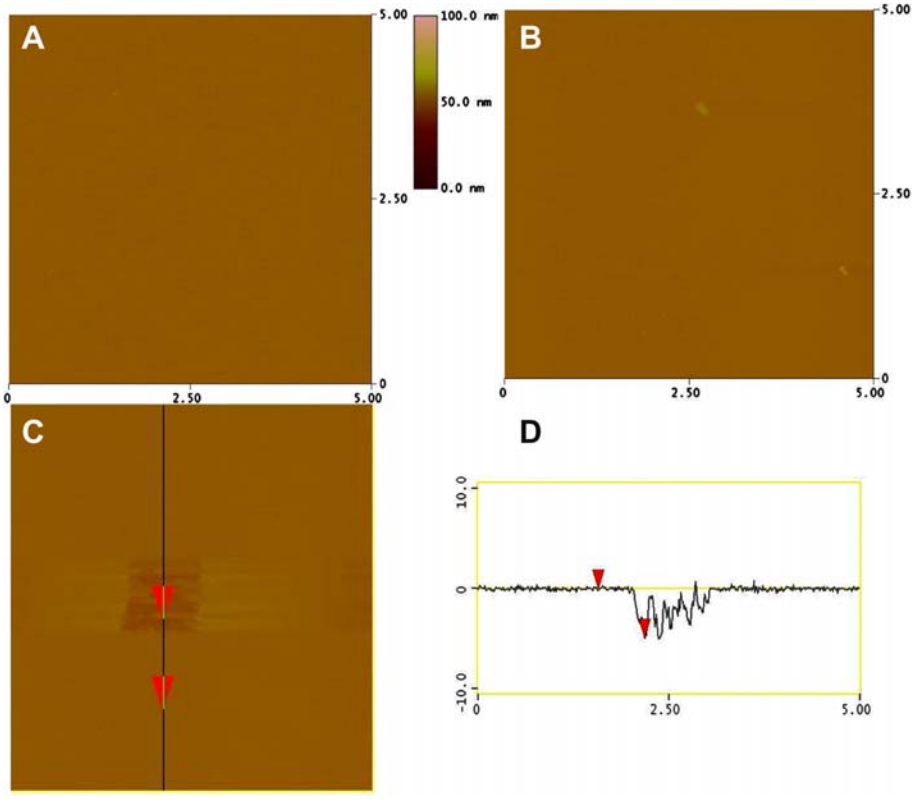


Fig. 2. AFM topography images of mica and mica-supported DOPC bilayers (scan size 5 μm × 5 μm). (A) Clean mica, (B) mica with lipid bilayers, (C) mica-supported DOPC bilayers with an artificial defect (1 μm × 1 μm area) under the increasing action force of AFM, (D) cross section analysis of (C).

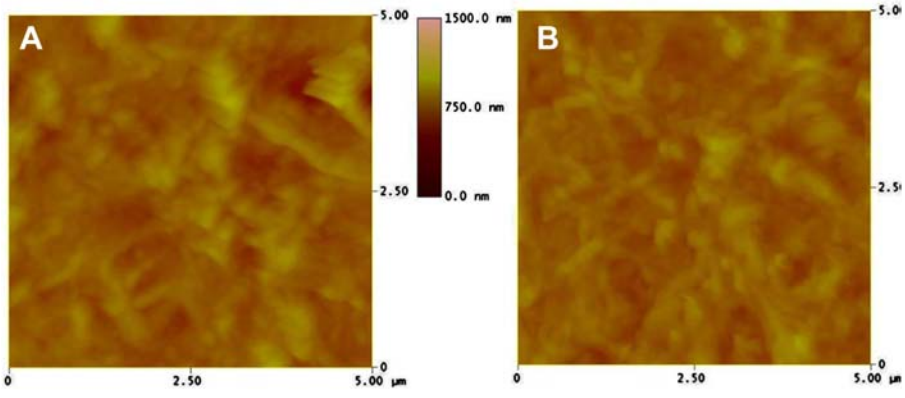


Fig. 3. AFM topography images of NF90- and NF90-supported DOPC bilayers (scan size 5 μm × 5 μm).

with the thickness of SPBs reported by other authors [29,30]. Then, we can conclude that DOPC SPBs with very few defects indeed is formed on mica by using vesicle fusion approach.

### 3.2. SPBs formed on NF membranes surface

In this work, four commercial NF membranes are used as substrates to prepare SPBs.

Fig. 3 shows AFM images of NF90 membrane and DOPC bilayers on NF90 membrane. The surface of NF90 membrane is very uneven and the roughness of NF90 membrane immersed in buffer solution is 55.460 nm (Fig. 3(A)). The roughness of DOPC bilayers is 44.776 nm (Fig. 3(B)). The decrease in the roughness value suggests the formation of DOPC bilayers on NF90 membrane. Although DOPC bilayers fills some uneven region of NF90 membrane surface, compared with mica-supported DOPC bilayers, SPBs on NF90 membrane surface exist more defects as shown in Fig. 3(B).

AFM images of NF270 membrane and DOPC bilayers on NF270 membrane are shown in Fig. 4. Large amount of round domains with different sizes are observed in Fig. 4(A). The NF270 membrane roughness is 8.136 nm, which is significantly less than that of the NF90 membrane. (Fig. 3(A)). It indicates that NF270 has better flatness than NF90. Fig. 4(B) shows the DOPC bilayers covered NF270 membrane.

It can be seen that the round domains disappear and the roughness further decreases to 3.747 nm, which indicates the formation of a more flat DOPC bilayers on NF270. Although round domains of NF270 membrane surface are filled by DOPC bilayers, compared with mica supported DOPC bilayers, SPBs on NF270 membrane surface exist certain defects as shown in Fig. 4(B).

Fig. 5 shows AFM images of NTR7250 membrane and DOPC bilayers on NTR7250 membrane. The surface topography of NTR7250 membrane contains many different sizes circles which exist large

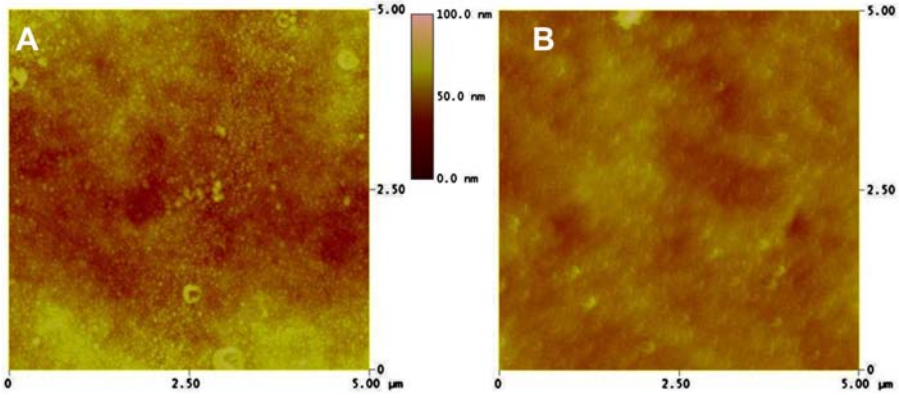


Fig. 4. AFM topography images of NF270- and NF270-supported DOPC bilayers (scan size 5 µm × 5 µm).

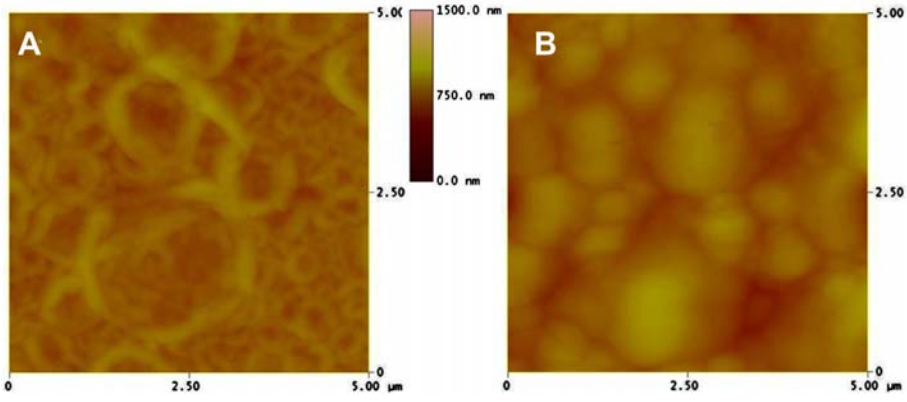


Fig. 5. AFM topography images of NTR7250- and NTR7250-supported DOPC bilayers (scan size 5 µm × 5 µm).

overlapping area and gaps between each other (Fig. 5 (A)). The roughness of NTR7250 membrane immersed in buffer solution is 43.200 nm, which is lower than NF90 membrane. That means the flatness of NTR7250 membrane surface is slightly better than NF90. Fig. 5 (B) shows the formation of DOPC bilayers on NTR7250 membrane. The circles on NTR7250 disappear and the large round domains appear. The roughness of NTR7250 membrane with phospholipid bilayers is 62.784 nm, which indicates the surface becomes more uneven. It may be caused by the formation of DOPC bilayers on the surface of NTR7250 membrane. The formation of DOPC bilayers covers the gap among overlapping circles of the NTR7250 membrane surface and emerges the accumulated round domains, which result in larger surface roughness and poor flatness. Furthermore, large defects of DOPC bilayers on NTR7250 membrane can be observed in Fig. 5(B). It also contributes to the increased roughness.

AFM images of NTR7450 membrane and DOPC bilayers on NTR7450 membrane are shown in Fig. 6. Fig. 6(A) shows the roughness of NTR7450 membrane is 1.743 nm, which is significantly less than that of the NF90, NF270, and NTR7250 membrane (Figs. 3(A), 4 (A), and 5(A)). The flatness of NTR7450 among four nanofiltration membrane is the highest, but there are also rugged regions. Fig. 6(B) shows that the DOPC bilayers cover NTR7450 membrane. It can be seen that some uneven areas disappear and the roughness further decreases to 1.172 nm, which indicates the formation of a more flat DOPC bilayers on NTR7450. In a word, SPBs have formed on the surface of NTR7450 membrane. The formation of SPBs covers uneven area of the NTR7450 membrane surface. The quality of SPBs on NTR7450 membrane surface is significantly superior to the rest NF membranes. Hence, operating conditions need to be optimized to form SPBs with few defects in the coming experiments. To certify the existence of SPBs on NTR7450, the action force of AFM scanning is increased. It can be seen that the formed SPBs is damaged under high AFM scanning force and the NTR7450 surface is exposed. The nick area of 1 μm × 1 μm is obtained (Fig. 6(C)). From the cross section image (Fig. 6(D)), it can be observed that the height of the DOPC layer is 4.397 nm. It is in good agreement with the thickness of SPBs reported by other authors [26,27]. Then, we can conclude that DOPC SPBs with very few defects indeed is formed on NTR7450 membrane surface by using vesicle fusion approach.

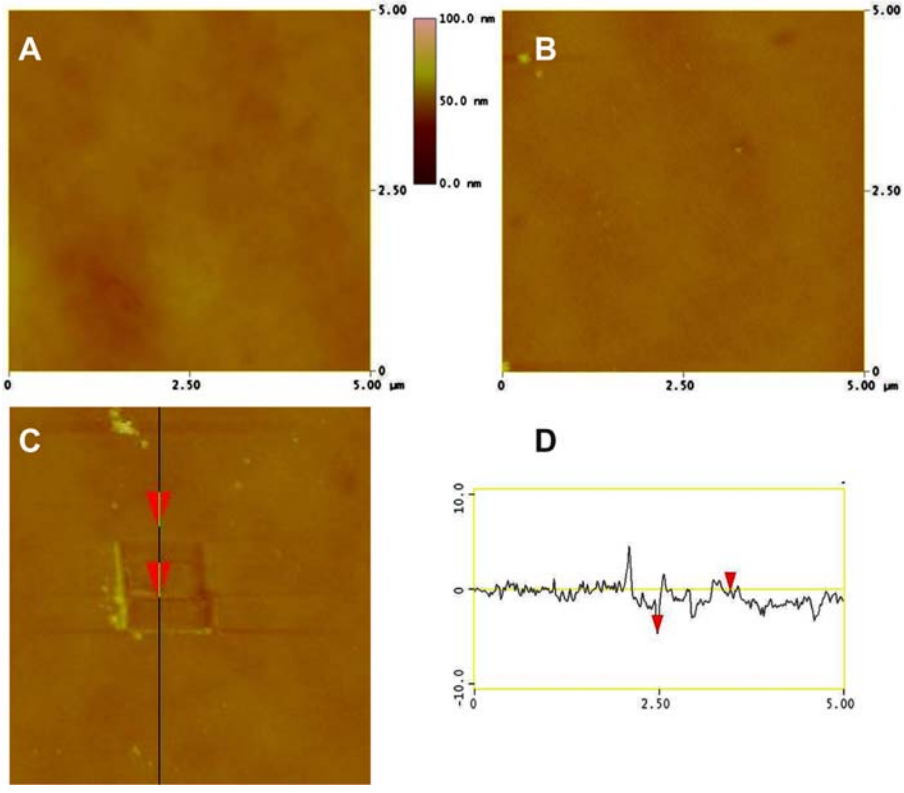


Fig. 6. AFM topography images of membranes (scan size 5 μm × 5 μm). (A) Clean NTR7450, (B) NTR7450-supported DOPC bilayers, (C) NTR7450-supported DOPC bilayers with an artificial defect (1 μm × 1 μm area) under the increasing action force of AFM, (D) cross section analysis of (C).

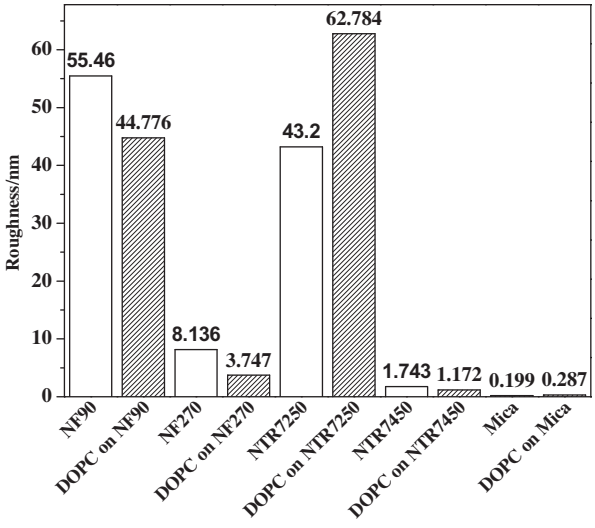


Fig. 7. Roughness of the different substrates surface.

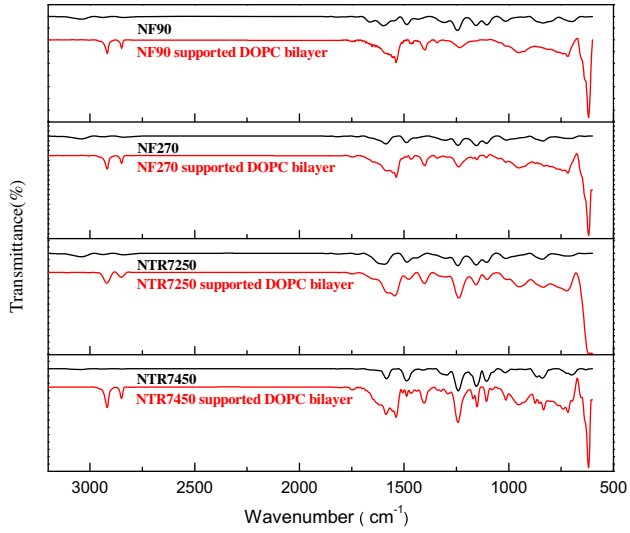


Fig. 8. FTIR spectra of four clean nanofiltration membranes (NF90, NF270, NTR7250, and NTR7450) and NF membranes–supported DOPC bilayers.

Fig. 7 shows the roughness of the different substrates surface. The roughness of NF90, NTR7250, NF270, NTR7450 membrane and mica in the Tris buffer solution successively reduce from 55.46 to 0.199 nm. The quality of DOPC bilayers is relevant to the roughness of the support membranes. Higher quality SPBs can be obtained on the membrane with lower roughness. As the roughness of NTR7450 membrane is similar to mica, NTR7450 membrane is most suitable to form SPBs among the four studied NF membranes.

### 3.3. *Attenuated total reflection Fourier transform infrared (ATR-FTIR)*

Fig. 8 exhibits the FTIR spectra of four different clean NF membranes and SPBs formed on NF membranes. As observed from the FTIR spectra, when DOPC bilayers deposit on NF membranes, the original peaks of NF membranes disappear and similar absorption peaks appear in all the four SPBs samples. Compared with the FTIR spectrum of pure DOPC sample (as shown in Fig. 9), the new peaks are consistent with DOPC characteristic peaks. That is to say DOPC bilayers can be obtained on all four NF membranes surface.

Fig. 9 exhibits the FTIR spectra of phospholipid bilayers membranes formed on four different nanofiltration membranes. Table 1 summarizes the assignments of the main IR bands of the spectra of Fig. 9. As observed from FTIR spectrum of Fig. 9, the peaks at 2917.63 and 2848.26 $cm^{-1}$ are in correspondence to $CH_2$ and $CH_3$ stretching vibrations, respectively [31].

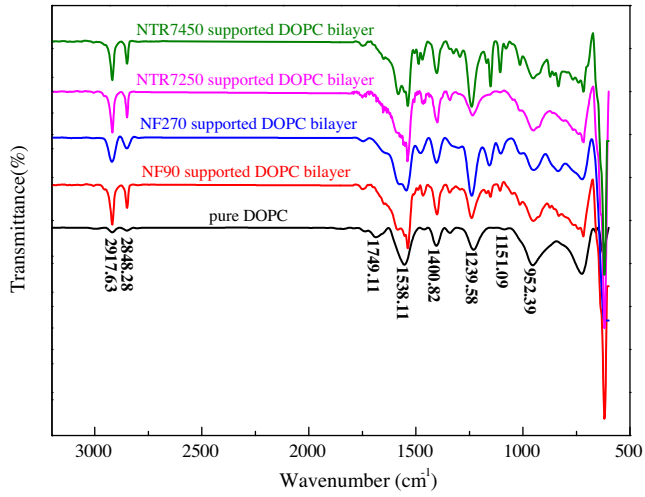


Fig. 9. The FTIR spectra of different NF membranes supported phospholipid bilayers and pure DOPC.

The peak at 1749.12 $cm^{-1}$ indicates the existence of carboxyl groups on phospholipid bilayers membranes. The peaks at 1538.11 and 1400.82 $cm^{-1}$ are associated with C=C stretching vibration [32–34] and C–H plane bending vibration in Olefin, respectively. The bands at 1239.58 and 1151.09 $cm^{-1}$ can be attributed to the asymmetric stretching vibrations of P=O and P–O–C. The peak at 952.39 $cm^{-1}$ can be assigned to the key-band of C–C–$N^+$ [35]. This confirms the attachment of the functional groups onto the phospholipid bilayers membranes, which can provide a large number of

Table 1
Wave numbers and assignments of the DOPC characteristic FTIR peaks

| Peak ($cm^{-1}$) | Assignment |
|---|---|
| 2917.63 | $–CH_2–$ stretching vibrations |
| 2848.28 | $–CH_3–$ stretching vibrations |
| 1749.11 | C=O stretching vibrations |
| 1538.11 1400.82 | C=C stretching vibrations C–H plane bending vibration in Olefin |
| 1239.58 | P=O asymmetric stretching vibrations |
| 1151.09 | P–O–C stretching vibrations |
| 952.39 | $C–C–N^+$ key band |

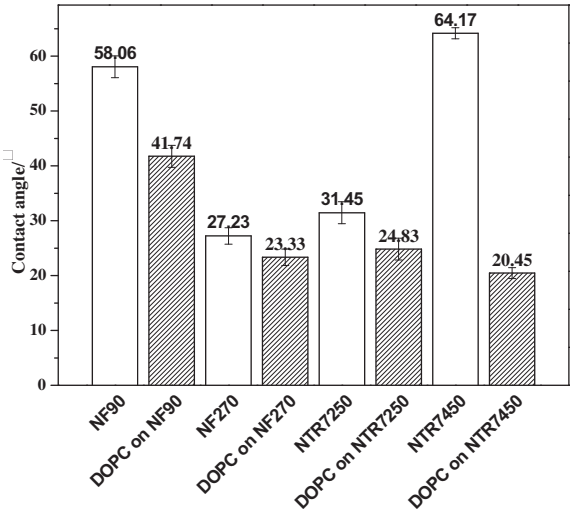


Fig. 10. Contact angle data of four different NF membranes and the NF membranes supported DOPC bilayers (Each data represents the mean ± standard deviation of seven samples).

chemical adsorption sites. It is certified that the SPBs indeed form on four different NF membranes.

### 3.4. Contact angle of SPBs on different substrate

Fig. 10 shows contact angle data of four different NF membranes and the NF membranes supported DOPC bilayers. The contact angle is an important parameter in measuring the surface hydrophobicity. In general, higher contact angle of the membrane surface indicates higher hydrophobicity [36,37]. As shown in Fig. 10, the contact angles of NF90, NF270, NTR7250, and NTR7450 are 58.06˚, 27.23˚, 31.45˚, and 64.17˚, respectively. The contact angles of NF90 and NTR7450 membranes are higher than those of the NF270 and NTR7250 membranes. According to the manufacturer, NF90 is a metaphenylene diamine (MPD)–based NF membrane, which shows low hydrophobicity. NF270 is a piperazine (PIP)-based NF membrane and its active layer is composed of cross-linked semi-aromatic polyamide. Its surface contains acidic $COO^-$ groups and some amine groups, which have strong interaction with water molecules. This character makes NF270 a good hydrophilic membrane. NTR7450 membrane has an active layer made of sulfonated polyethersulfone. NTR7250 membrane is a composite NF membrane that contains carbonyl and hydroxyl groups. More hydrophilic groups of NTR7250 membrane lead to lower contact angle than that of NTR7450 membrane.

The contact angles of the DOPC bilayers deposited NF90, NF270, NTR7250, and NTR7450 membranes decrease to 41.74˚, 23.33˚, 24.83˚, and 20.45˚ respectively. The remarkable reduction in the contact angle suggests the formation of SPBs on different NF membranes. As shown in Fig. 10, NF90-supported DOPC membrane shows the highest contact angle. Combined with the AFM images (Fig. 3), it can be concluded that the NF90 DOPC bilayers have many defects due to the high roughness and poor hydrophilicity of NF90 membrane. As NF270 exhibits both good flatness and hydrophilicity, high-quality DOPC SPBs with few defects can be observed on NF270 surface. However, NTR7250 have high roughness and good hydrophilicity. On the contrary, NTR7450 shows excellent flatness and highest hydrophobicity. With AFM images of DOPC bilayers on NTR7250 (Fig. 5) and NTR7450 (Fig. 6), it is easy to see that the defect-free DOPC SPBs with excellent hydrophilicity can be obtained on NTR7450 surface. The NTR-7450 surface is noticeably the smoothest and most homogeneous among the four NF membranes. Meanwhile, the top layer of NTR-7450 membrane surface is dense and virtually impermeable to lipids and proteins. Therefore, NTR7450 membrane is the most suitable substrate to form SPBs. To sum up, the SPBs spread easily on the smooth and hydrophilic surface. Moreover, the flatness of the membrane surface is the primary factor to determine the quality of SPBs.

## 4. Conclusions

This article describes the feasibility of covering a NF membrane with a continuous phospholipid bilayers using the vesicle fusion approach. The surface topography, functionalized groups of SPBs and contact angle on different substrates are characterized by AFM, ATR-FTIR, and contact angle measurement techniques.

AFM images reveal that homogeneous NF membranes surface are crucial for successful the formation of SPBs with very few defects. Phospholipid can be spread in a variety NF membrane surfaces. The roughness of the SPBs on NTR7450 membrane surface is lowest among four NF membranes. NTR7450 membrane is the most suitable to form SPBs among four NF membranes. FTIR spectra confirm the attachment of the functional groups onto the phospholipid bilayers membranes. The contact angles reveal the formed SPBs on NF membranes surface increases the hydrophilicity of membrane surface. The flatness of the membrane surface is the primary factor to determine the quality of SPBs compared with the hydrophilicity of the membrane surface.

## Acknowledgments

The authors are grateful to the financial support from the National Basic Research Program of China (No. 2009CB623402), National Natural Science Foundation of China (No. 21106139), Doctoral Fund of Ministry of Education of China (No. 20110132120026), and Excellent Young Scientist Research Award Fund of Shandong Province (No. BS2011CL040).

## References

[1] G. Yasmine, T. Safia, R. Amina, S. Samia, G. Noreddine, Physical and chemical assessment of MSF distillate and SWRO product for drinking purpose, Desalination 290 (2012) 107–114.
[2] D. Li, H.T. Wang, Recent developments in reverse osmosis desalination membranes, J. Mater. Chem. 20 (2010) 4551–4566.
[3] N.N. Li, Separation science and technology in the 21st century-from an industrial perspective of energy, sustainability and globalization. 2009 AIChE Annual Meeting, Nashville, TN, 2009, Nov. 8–13.
[4] E. Sackmann, Supported membranes: scientific and practical applications, Science 271 (1996) 43–48.
[5] A.L. Plant, Supported hybrid bilayer membranes as rugged cell membrane mimics, Langmuir 15 (1999) 5128–5135.
[6] S.G. Boxer, Molecular transport and organization in supported lipid membranes, Curr. Opin. Chem. Biol. 4 (2000) 704–709.
[7] A.R. Sapuri, M.M. Baksh, J.T. Groves, Electrostatically targeted intermembrane lipid exchange with micropatterned supported membranes, Langmuir 19 (2003) 1606–1610.
[8] W. Knolla, H. Parka, E.K. Sinnerb, D. Yao, Y. Fang, Supramolecular interfacial architectures for optical biosensing with surface plasmons, Prog. Surf. Sci. 570 (2004) 30–42.
[9] P. Mueller, D.O. Rudin, H.T. Tien, Reconstitution of cell membrane structure *in vitro* and its transformation into an excitable system, Nature 194 (1962) 979–980.
[10] P. Muller, D. Rudin, Methods for the formation of single bimolecular lipid membranes in aqueous solution, Prog. Surf. Sci. 67 (1963) 534–539.
[11] M.S. Mauter, M. Elimelech, Environmental applications of carbon-based nano-materials, Environ. Sci. Technol. 42 (2008) 5842–5859.
[12] A. Noy, H.G. Park, F. Fornasiero, J.K. Holt, C.P. Grigoropoulos, O. Bakajin, Nanofluidics in carbon nanotubes, Nano Today 6 (2007) 22–29.
[13] P. Agre, Membrane water transport and aquaporins: looking back, Bio. Cell 97 (2005) 355–356.
[14] M. Kumar, M. Grzelakowski, J. Zilles, M. Clark, W. Meier, Highly permeable polymeric membranes based on the incorporation of the functional water channel protein Aquaporin Z, Proc. Natl. Acad. Sci. 104 (2007) 20719–20724.
[15] G.P. Alfredo, K.B. Stibius, V. Thomas, C.H. Nielsen, O.G. Mouritsen, Biomimetic triblock copolymer membrane arrays: a stable template for functional membrane proteins, Langmuir 25 (2009) 10447–10450.
[16] A. Taubert, Controlling water transport through artificial polymerprotein hybrid membranes, Proc. Natl. Acad. Sci. 104 (2007) 20643–20644.
[17] S. Garcia-Manyes, G. Oncins, F. Sanz, Effect of ion-binding and chemical phospholipid structure on the nanomechanics of lipid bilayers studied by force spectroscopy, Biophy. J. 89 (2005) 1812–1826.
[18] P. Xua, J.E. Drewesa, T. Kimb, C. Bellonaa, G. Amyc, Effect of membrane fouling on transport of organic contaminants in NF/RO membrane applications, J. Membr. Sci. 279 (2006) 165–175.
[19] S. Garcia-Manyes, G. Oncins, F. Sanz, Effect of pH and ionic strength on phospholipid nanomechanics and on deposition process onto hydrophilic surfaces measured by AFM, Electrochim. Acta 51 (2006) 5029–5036.
[20] Y. Kaufman, A. Berman, V. Freger, Supported lipid bilayer membranes for water purification by reverse osmosis, Langmuir 26 (2010) 7388–7395.
[21] V. Freger, Nanoscale heterogeneity of polyamide membranes formed by interfacial polymerization, Langmuir 19 (2003) 4791–4797.
[22] V. Freger, Swelling and morphology of the skin layer of polyamide composite membranes an atomic force microscopy study, Environ. Sci. Technol. 38 (2004) 3168–3175.
[23] R. Du, A. Chakma, X. Feng, Interfacially formed poly (N, N-dimethyla-minoethyl methacrylate)/polysulfone composite membranes for $CO_2/N_2$ separation, J. Membr. Sci. 290 (2007) 19–28.
[24] A.R. Roudman, F.A. DiGiano, Surface energy of experimental and commercial nanofiltration membranes: effects of wetting and natural organic matter fouling, J. Membr. Sci. 175 (2000) 61–73.
[25] J. Schaep, C. Vandecasteele, Evaluating the charge of nanofiltration membranes, J. Membr. Sci. 188 (2001) 129–136.
[26] T. Kiwada, K. Sonomura, Y. Sugiura, K. Asami, S. Futaki, Transmission of extramembrane conformational change into current: construction of metal-gated ion channel, J. Am. Chem. Soc. 128 (2006) 6010–6011.
[27] N. Sakai, J. Mareda, S. Matile, Artificial beta-barrels, Acc. Chem. Res. 41 (2008) 1354–1365.
[28] V. Freger, S. Srebnik, Mathematical model of charge and density distributions in interfacial polymerization of thin films, J. Appl. Polym. Sci. 88 (2003) 1162–1169.
[29] A.M. Mika, R.F. Childs, Salt separation by charged gel-filled microporous membranes, Ind. Eng. Chem. Res 42 (2003) 3111–3117.
[30] M. Manttari, A. Pihlajamaki, M. Nystrom, Effect of pH on hydrophilicity and charge and their effect on the filtration efficiency of NF membranes at different pH, J. Membr. Sci. 280 (2006) 311–0320.
[31] Y.L. Cheng, N. Boden, R.J. Bushby, S. Clarkson, S.D. Evans, P.F. Knowles, A. Marsh, B. Mills, Attenuated total reflection fourier transform infrared spectroscopic characterization of fluid lipid bilayers tethered to solid supports, Langmuir 14 (1998) 839–844.
[32] R. Sepahvand, M. Adeli, B. Astinchap, R. Kabiri, New nanocomposites containing metal nanoparticles, carbon nanotube and polymer, J. Nanopart. Res. 10 (2008) 1309–1318.
[33] S.T. Yang, J.X. Li, D.D. Shao, J. Hu, X.K. Wang, Adsorption of Ni(II) on oxidized multi-walled carbon nanotubes: effect of contact time, pH, foreign ions and PAA, J. Hazard. Mater. 166 (2009) 109–116.

[34] V. Vatanpoura, S.S. Madaenia, R. Moradianb, S. Zinadinia, B. Astinchap, Fabrication and characterization of novel antifouling nanofiltration membrane prepared from oxidized multiwalled carbon nanotube/polyethersulfone nanocomposite, J. Membr. Sci. 375 (2011) 284–294.
[35] M.R. Hernandez, E.N. Towns, J. Moore, H. Lee, J.B. German, C.B. Lebrilla, A.N. Parikh, D.P. Land, Use of attenuated total reflectance Fourier transform infrared spectroscopy to study lactosylceramide and GD3 DMPC bilayers, Colloids Surf., B: Biointerfaces 94 (2012) 374–377.
[36] L. Palacio, J.I. Calvo, P. Prádanos, A. Hernández, P. Väisänen, M. Nyström, Contact angles and external protein adsorption onto UF membranes, J. Membr. Sci. 152 (1999) 189–201.
[37] J.T.F. Keurentjes, J.G. Harbrecht, D. Brinkman, J.H. Hanemaaijer, S.M.A. Cohen, R.K. Van't, Hydrophobicity measurements of microfiltration and ultrafiltration membranes, J. Membr. Sci. 47 (1989) 333–344.